The Astrophysical Journal Letters, 739:L54 (6pp), 2011 October 1 doi:10.1088/2041-8205/739/2/L54

THE FLUORINE DESTRUCTION IN STARS: FIRST EXPERIMENTAL STUDY OF THE ^{19}F(p, α_0)^{16}O REACTION AT ASTROPHYSICAL ENERGIES

M. La Cognata[1], A. M. Mukhamedzhanov[2], C. Spitaleri[1,3], I. Indelicato[1,3], M. Aliotta[4], V. Burjan[5], S. Cherubini[1,3], A. Coc[6], M. Gulino[1,3], Z. Hons[5], G. G. Kiss[1], V. Kroha[5], L. Lamia[1,3], J. Mrázek[5], S. Palmerini[7], Š. Piskoř[5], R. G. Pizzone[1], S. M. R. Puglia[1,3], G. G. Rapisarda[1,3], S. Romano[1,3], M. L. Sergi[1,3], and A. Tumino[1,8]

[1] INFN-Laboratori Nazionali del Sud, Catania, Italy; lacognata@lns.infn.it
[2] Cyclotron Institute-Texas A&M University, College Station, TX, USA
[3] Dipartimento di Fisica e Astronomia-Università di Catania, Catania, Italy
[4] School of Physics and Astronomy, University of Edinburgh, Edinburgh, and SUPA-Scottish Universities Physics Alliance, UK
[5] Nuclear Physics Institute of ASCR, Rez near Prague, Czech Republic
[6] CSNSM CNRS/IN2P3, Université Paris Sud, Orsay, France
[7] Dipartimento di Fisica-Università di Perugia, and INFN-Sezione di Perugia, Perugia, Italy
[8] Facoltà di Ingegneria e Architettura, Università degli Studi di Enna "Kore," Enna, Italy
Received 2011 June 30; accepted 2011 July 28; published 2011 September 9

ABSTRACT

The ^{19}F(p, α)^{16}O reaction is an important fluorine destruction channel in the proton-rich outer layers of asymptotic giant branch (AGB) stars and it might also play a role in hydrogen-deficient post-AGB star nucleosynthesis. So far, available direct measurements do not reach the energy region of astrophysical interest ($E_{\rm cm} \lesssim 300$ keV), because of the hindrance effect of the Coulomb barrier. The Trojan Horse (TH) method was thus used to access this energy region, by extracting the quasi-free contribution to the ^{2}H(^{19}F, α^{16}O)n and the ^{19}F(^{3}He, α^{16}O)d reactions. The TH measurement of the α_0 channel shows the presence of resonant structures not observed before, which cause an increase of the reaction rate at astrophysical temperatures up to a factor of 1.7, with potential consequences for stellar nucleosynthesis.

Key words: nuclear reactions, nucleosynthesis, abundances – stars: abundances – stars: AGB and post-AGB

Online-only material: color figures

1. ASTROPHYSICAL MOTIVATIONS

Fluorine is a key element for astrophysics. Its abundance is very sensitive to the physical conditions within stars and for such a reason it is used to probe hotly debated nucleosynthesis scenarios (Lucatello et al. 2011). The most likely environments where its production can take place in the Milky Way are: during core collapse of Type II supernovae (Woosley & Haxton 1988) through the ν-process, in Wolf–Rayet stars (Meynet & Arnould 2000), and in the convective zone generated by a thermal pulse in asymptotic giant branch (AGB) stars (Cristallo et al. 2009). Recently, fluorine overabundances by factors of 800–8000 (Pandey et al. 2008) have been observed in R-Coronae-Borealis stars and provide evidence for the synthesis of fluorine in such hydrogen-deficient supergiants. Yet, despite its key importance, a detailed description of fluorine nucleosynthesis is still missing.

In AGB stars, regarded as the major contributors to the Galactic fluorine (Jorissen et al. 1992), the largest observed fluorine overabundances cannot be explained with standard AGB models and required additional mixing (Lugaro et al. 2004). A possible lack of proper accounting for the contribution from C-bearing molecules (i.e., CH, CN, CO, and C2) might provide an interpretation in Population I stars (Abia et al. 2010), by providing a renormalization of the observed abundances, though the understanding of F production in the case of metal-poor AGB stars is far from satisfactory (Lucatello et al. 2011). An alternative justification could be given by a reassessment of the nuclear reaction rates involved in fluorine production and destruction. For example, deep mixing phenomena in AGB stars can alter the stellar outer-layer isotopic composition due to proton capture at low temperatures ($T_9 \lesssim 0.04$), affecting the transported material (Nollett et al. 2003; Sergi et al. 2010; Busso et al. 2010). In this environment, the ^{19}F(p, α)^{16}O reaction at $E_{\rm cm} \sim 27$–94 keV (corresponding to the Gamow window; Rolfs & Rodney 1988) would represent the main fluorine destruction channel, possibly modifying F surface abundances, as proposed by Lucatello et al. (2011) and Abia et al. (2011).

In the case of hydrogen-deficient post-AGB stars, Clayton et al. (2007) have shown that hydrogen admixture (if the CO white dwarf retained a small H-rich envelope) plays a key role to reverse the effect of excessive He burning and yields elemental abundances in better agreement with observations. Here, the ^{19}F(p, α)^{16}O reaction might bear a great importance as it would remove both protons and F nuclei from the nucleosynthesis scenario. Since the temperature at the base of the accreted material approaches $T_9 \sim 0.2$ (Pandey et al. 2008), the ^{19}F(p, α)^{16}O cross section should be known at $E_{\rm cm} \sim 50$–300 keV for accurate modeling.

2. AVAILABLE DIRECT DATA AND SPECTROSCOPIC INFORMATION

Proton-induced ^{19}F destruction has been the subject of several experimental investigations, because of its astrophysical and spectroscopic relevance.

As pointed out in the Nuclear Astrophysics Compilation of Reaction Rates (NACRE; Angulo et al. 1999) and confirmed by Spyrou et al. (2000), the ^{19}F(p, α_0)^{16}O channel is giving the largest contribution to the reaction rate of the ^{19}F(p, α)^{16}O reaction for $0.01 < T_9 < 0.1$. In the NACRE compilation, the recommended ^{19}F(p, α_0)^{16}O astrophysical S(E)-factor was obtained from several works (Breuer 1959; Warsh et al. 1963; Caracciolo et al. 1974; Cuzzocrea et al. 1980; Isoya et al. 1958; Morita et al. 1966), with the lowest-energy direct data reaching 461 keV center-of-mass (c.m.) energy (Breuer 1959). The Gamow window is only partially covered by the unpublished data of Lorentz-Wirzba (1978), which have been used in Herndl et al. (1991) and Yamashita & Kudo (1993) to evaluate the astrophysical factor in the zero- and finite-range Distorted Wave Born Approximation (DWBA) approaches, respectively. These data support a strong suppression of compound ^{20}Ne decay to the ground state of ^{16}O at $E_{\rm cm} \sim 0.14$–0.6 MeV. However, these results were not included in the NACRE compilation as possible systematic errors affecting the absolute normalization might lead to an underestimate of S(E) by a factor of two (Angulo et al. 1999). The astrophysical factor was then extrapolated to low energies assuming a dominant contribution of the non-resonant part (Angulo et al. 1999). This conclusion disagrees with older measurements in Breuer (1959), where the existence of two resonances with $J^\pi = 1^-$ and 0^+ had been reported at $E_{\rm cm} \sim 0.4$ MeV. It is worth noting that additional resonances might be populated in ^{20}Ne as they are permitted by their quantum numbers (Tilley et al. 1998).

In conclusion, the available experimental data have allowed the computation of the rate for $T_9 > 0.3$. Below this temperature, the rate is determined mainly from the non-resonant (p, α_0) channel, causing a progressive increase of the uncertainties up to ∼50% at the lowest temperatures (Angulo et al. 1999).

To ascertain the actual contribution of resonances at astrophysical energies and evaluate their impact on astrophysics, an experimental program has been set forth to measure the ^{19}F$(p, \alpha)^{16}$O astrophysical S(E)-factor by means of the Trojan Horse (TH) method.

3. THE TH THEORY: THE MODIFIED *R*-MATRIX APPROACH

The TH method has been developed in the early 1990s with the aim of measuring low-energy nuclear reactions unhindered by the Coulomb barrier (Baur 1986; Cherubini et al. 1996; Spitaleri et al. 1999; La Cognata et al. 2008). Since then it has been successfully applied to several reactions of astrophysical interest. Recently, a generalized *R*-matrix approach has been developed (Mukhamedzhanov et al. 2007; La Cognata et al. 2007, 2010a, 2010b; Mukhamedzhanov et al. 2008) to analyze multiresonance TH reactions. This differs from standard *R*-matrix (Lane & Thomas 1958) as it considers the half-off-energy-shell character of the TH cross section. Let us consider the TH reaction

$$a + A \rightarrow s + c + C, \quad (1)$$

where $a = (s\,x)$. This TH reaction is used to obtain the astrophysical factor for the resonant subreaction

$$x + A \rightarrow c + C. \quad (2)$$

If the cluster s escapes without interacting with the $x+A$ system (quasi-free (QF) condition), the TH reaction amplitude is given by an expression similar to the binary resonant reaction amplitude (see Equation (10) in La Cognata et al. 2010a). In details, it contains the overlap function $I^F_{A\,\tau} = \langle \Phi_\tau | \varphi_A \rangle$ of the internal wave function of the system $F = x + A = c + C$ excited to the level τ and the bound-state wave function of A. This can be parameterized in terms of the boundary condition in the channel $x+A$ and of the reduced width amplitude $\gamma_{xA\,\tau}$, as the *R*-matrix amplitude for the binary resonant reaction $x + A \rightarrow c + C$ proceeding through the resonance state F_τ (A. Mukhamedzhanov 2011, in preparation). Assuming non-interfering resonances, the TH cross section is obtained in the plane-wave (PW) approximation:

$$\frac{d^2\sigma}{dE_{xA}d\Omega_s} = \mathrm{NF} \sum_\tau (2J_\tau + 1) \times \left| \sqrt{\frac{k_f(E_{xA})}{\mu_{cC}}} \frac{\sqrt{2P_{l_\tau}(k_{cC}R_{cC})}M_\tau(p_{xA}R_{xA})\gamma_{cC\,\tau}\gamma_{xA\,\tau}}{D_\tau(E_{xA})} \right|^2 . \quad (3)$$

Here, NF is a normalization factor, J_τ the spin of the τth resonance, $k_f(E_{xA}) = \sqrt{2\mu_{cC}(E_{xA} + Q)}/\hbar$ (Q is the Q-value of reaction 2, E_{xA} the x–A-relative energy), P_{l_τ} is the penetration factor in l_τ-wave, R_{xA} and R_{cC} are the channel radii.

$$M_\tau(p_{xA}R_{xA}) = \left[(B_{xA\,\tau} - 1)\, j_{l_\tau}(\rho) - \rho \frac{\partial j_{l_\tau}(\rho)}{\partial \rho} \right]_{\rho = p_{xA}\,R_{xA}} , \quad (4)$$

where $j_{l_\tau}(\rho)$ is the spherical Bessel function, $p_{xA} = \sqrt{2\mu_{xA}(E_{xA} + B_{xs})}/\hbar$ (B_{xs} is the binding energy of the $a = (x\,s)$ system), and $B_{xA\,\tau}$ an arbitrary boundary condition chosen as in La Cognata et al. (2010a) to yield the observable resonance parameters. Finally, $D_\tau(E_{xA})$ is the standard *R*-matrix denominator in the case of two-level, one-channel *R*-matrix formulae (Lane & Thomas 1958), containing shift and penetration functions besides the boundary conditions set as above.

4. MEASUREMENT AND RESULTS

Two experimental runs were performed, using two different TH nuclei to transfer the participant proton. In the first run, the QF ^{2}H$(^{19}$F$, \alpha^{16}$O$)n$ reaction at 50 MeV beam energy was measured, in the second the ^{19}F$(^3$He$, \alpha^{16}$O$)d$ reaction at $E_{\rm beam} = 18.2$ MeV (to check for pole invariance; Pizzone et al. 2011). In what follows we will focus on the measurement of the ^{19}F$(p, \alpha_0)^{16}$O astrophysical factor and we will describe the first run only (where the spectator s is the neutron); the experimental setups were similar in the two experiments. A 1 mm collimated ^{19}F beam impinged onto deuterated polyethylene (CD2) targets (∼100 μg cm^{-2} thick). The experimental setup comprised a $\Delta E - E$ telescope, consisting of an ionization chamber and a silicon position sensitive detector (PSD1) on one side of the scattering chamber and four additional silicon PSDs (PSD2-5) on the opposite side of the beam axis. The $\Delta E - E$ telescope was optimized for the detection of ^{16}O recoils, while the PSDs for coincident detection of the α-particles. Angular conditions were selected to optimize the QF contribution. Channel selection was accomplished by gating on the $\Delta E - E$ spectra to select the $Z = 8$ locus and on the Q-value of the ^{2}H$(^{19}$F$, \alpha_0{}^{16}$O$)n$ reaction.

Compelling evidence for the occurrence of the QF mechanism is provided by the observed agreement between the experimental p–n momentum distribution inside the deuteron and the theoretical one given by the square of the Hulthén wave function in momentum space (in the PW approximation; Spitaleri et al. 1999; Pizzone et al. 2009). Since this is a necessary condition for the QF mechanism being present and dominant, only events satisfying the condition $0 < p_n < 40$ MeV c^{-1} for the neutron momentum range, where the agreement is observed ($\tilde{\chi}^2 = 1.4$), are considered in the extraction of the QF cross section $d^3\sigma/dE_{\rm cm}d\Omega_{\rm cm}d\Omega_n$ of the ^{2}H$(^{19}$F$, \alpha_0{}^{16}$O$)n$ reaction. A minor background contribution was identified as being

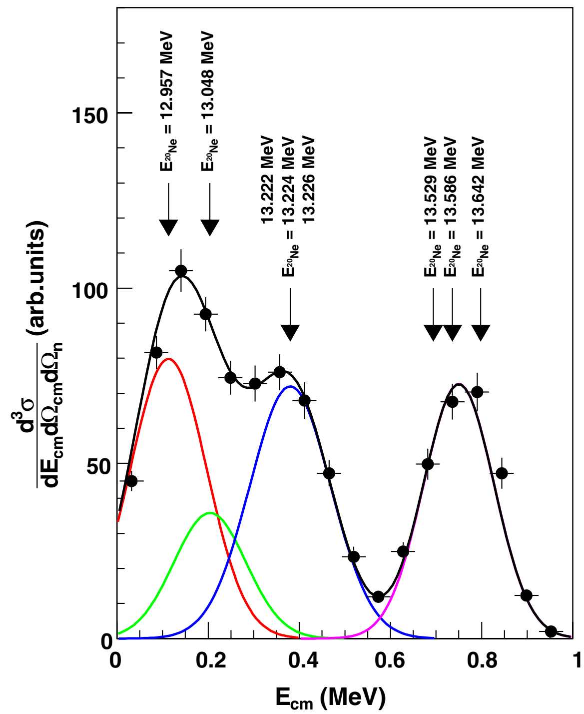

Figure 1. Normalized coincidence yield of the ^{2}H(^{19}F, $\alpha_0{}^{16}$O)n reaction. The black circles are the experimental data, with the horizontal error bars defining the $p - {}^{19}$F-relative-energy binning used in data reduction and the vertical ones the statistical uncertainties. The black line is a multi-Gaussian fitting of the experimental data. The red and green lines are the contributions of the 12.957 and 13.048 MeV ^{20}Ne levels, respectively. The blue line describes the combined yield of the 13.222, 13.224, and 13.226 MeV states while the purple line one of the 13.529, 13.586, and 13.642 MeV levels, as marked by the arrows.

(A color version of this figure is available in the online journal.)

due to the $^{2}\mathrm{H} + {}^{19}\mathrm{F} \rightarrow \alpha + {}^{17}\mathrm{O} \rightarrow \alpha + {}^{16}\mathrm{O} + n$ sequential decay. Such contribution represents ∼7% of the gated coincidence yield in the $p - {}^{19}$F relative-energy range $E_{\mathrm{cm}} = 0$–1 MeV and was subtracted by fitting the $E_{n-{}^{16}\mathrm{O}}$ relative-energy spectrum. A similar discussion applies to the ^{19}F(^{3}He, α^{16}O)d reaction. Anyway, too low statistics prevented us to extract angular distributions as well as the TH cross section from this data set.

The normalized coincidence yield is given in Figure 1. It was obtained by dividing the selected coincidence yield by the product of the phase-space factor and of the p–n momentum distribution (see La Cognata et al. 2010a, 2010b, and references therein). The experimental data clearly show the presence of three resonance groups corresponding to ^{20}Ne states at 12.957 and 13.048 MeV; 13.222, 13.224, and 13.226 MeV; and 13.529, 13.586, and 13.642 MeV. The normalized yield was fitted simultaneously with four Gaussian curves to separate the resonance contributions. In Figure 1 the multi-Gaussian fitting curve is shown by a black line, the red and green lines outline the contribution of the 12.957 and 13.048 MeV ^{20}Ne levels, respectively, the blue line describes the combined yield of the 13.222, 13.224, and 13.226 MeV states while the purple line the one of the 13.529, 13.586, and 13.642 MeV levels. A single Gaussian was used in these last two cases as the 13.222, 13.224, and 13.226 MeV levels could not be resolved in the experimental E_{cm} spectrum and because the 13.529, 13.586, and 13.642 MeV levels have the same spin parity (Tilley et al. 1998). Such a separation was needed to integrate the $d^3\sigma/d\Omega_{\mathrm{cm}}dE_{\mathrm{cm}}d\Omega_n$ cross section over the α emission angle in the c.m. system of the subreaction ^{19}F(p, α_0)^{16}O (La Cognata et al. 2010b). Since the

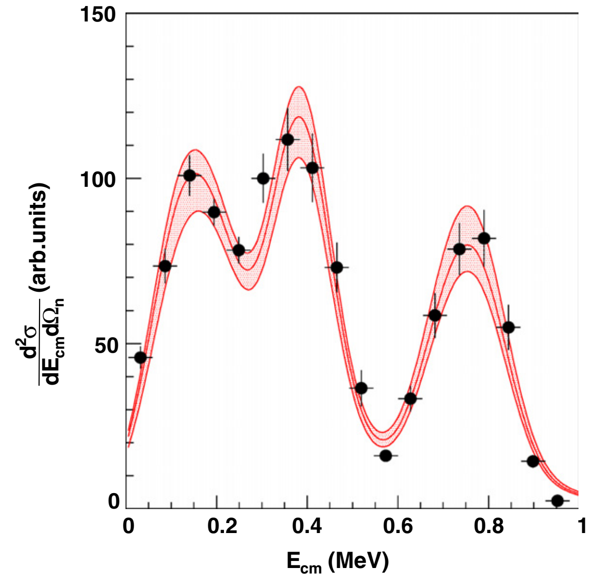

Figure 2. QF cross section of the ^{2}H(^{19}F, $\alpha_0{}^{16}$O)n reaction in arbitrary units. The black circles are the experimental data, with the horizontal error bars defining the $p - {}^{19}$F-relative-energy binning. The vertical error bars account for the statistical and angular-distribution integration uncertainties. The cross section was calculated in the modified R-matrix approach (Equation (3)), normalized to the peak at about 750 keV and convoluted with the experimental resolution. The middle line represents the best fit to the data, the upper and lower limits of the uncertainty range accounting for statistical and normalization errors.

(A color version of this figure is available in the online journal.)

experimental θ_{cm} range spans ∼70°–110°, angular distributions outside this angular interval were calculated by means of the general expression for resonance reactions obtained by Blatt & Biedenharn (1952; La Cognata et al. 2010b). In the integration, the $J^\pi = 3^- E_R = 13.226$ MeV state in ^{20}Ne was assumed to dominate over the two neighbor resonances, because of the $2J_\tau+1$ enhancement factor in each term of the modified R-matrix formula (Equation (3); La Cognata et al. 2010a). Under this assumption, an upper limit of the experimental $d^2\sigma/dE_{\mathrm{cm}}d\Omega_n$ cross section is obtained in the $E_{\mathrm{cm}} \sim 0.3$–0.5 MeV region.

The total TH cross section $d^2\sigma/dE_{\mathrm{cm}}d\Omega_n$ is displayed in Figure 2 as full dots. Statistical uncertainties and those due to angular-distribution integration are given, as the other source of uncertainty, namely background subtraction, contributes by less than 20% to the total error budget. The horizontal error bars give the width of the $p - {}^{19}$F relative-energy bins used in the data analysis. The experimental TH cross section was analyzed in the modified R-matrix approach (Equation (3) and La Cognata et al. 2010a). As a first step, a weighed fit of the direct astrophysical S(E)-factor data available in the literature, down to about 0.6 MeV (Angulo et al. 1999), was performed by means of standard R-matrix formulae. This is needed to extract the reduced γ-widths of the measured 13.529, 13.586, and 13.642 MeV states in ^{20}Ne, to be inserted into the modified R-matrix fitting. The resulting p- and α-reduced widths (γ_p and γ_{α_0}) are given in Table 1. The TH measurement has been extended up to 1 MeV for normalization to the direct astrophysical factor. The normalization factor was then determined by scaling the calculated $d^2\sigma/dE_{\mathrm{cm}}d\Omega_n$ to the experimental TH cross section in the overlap region between direct and indirect data, namely to the peak at about 0.75 MeV. Therefore, the reduced widths of the lower energy resonances obtained with the modified R-matrix fit are normalized to the

Table 1
Reduced and Observable Partial Widths from *R*-matrix Fits

E_R (MeV)	J^π	γ_p ($\mathrm{MeV}^{1/2}$)	γ_{α_0} ($\mathrm{MeV}^{1/2}$)	Γ_p (MeV)	Γ_{α_0} (MeV)
From modified *R*-matrix (Equation (3))					
12.957	2^+	$0.110^{+0.007}_{-0.012}$	0.068	$(9.6^{+1.2}_{-2.0}) \times 10^{-12}$	0.038
13.048	4^+	$0.690^{+0.069}_{-0.049}$	0.0446	$(1.22^{+0.14}_{-0.17}) \times 10^{-11}$	0.010
13.222[a]	0^+	...	...	...	...
13.224[a]	1^-	...	...	...	...
13.226	3^-	$0.305^{+0.020}_{-0.026}$	0.086	$(8.1^{+1.0}_{-1.4}) \times 10^{-8}$	0.053
From standard *R*-matrix (Lane & Thomas 1958)					
13.529	2^+	0.0410	0.0561		
13.586	2^+	0.0825	0.0904		
13.642	2^{+b}	0.0581	0.0467		

Notes. Resonance energies, spin parities, and α_0 partial widths are fixed to the values in the literature (Tilley et al. 1998) in the modified *R*-matrix fitting.
[a] The contribution of these resonances is assumed to be negligible in the fitting.
[b] The spin-parity assignment to this resonance is ambiguous, also $J^\pi = 0^+$ is reported (Tilley et al. 1998).

ones of the 13.529, 13.586, and 13.642 MeV ^{20}Ne states. The normalization error accounts for reduced widths of these states different from the ones in Table 1, but still leading to an S(E)-factor in agreement with the direct one within the quoted uncertainties. The experimental energy resolution was accounted for by smearing the calculated TH cross section to match the shape of the peak at about 0.75 MeV. Such a procedure, described in La Cognata et al. (2009), yielded an energy resolution of 60 keV. The normalized γ_p and γ_{α_0} are listed in Table 1. In the calculation, the Γ_{α_0} partial widths, being essentially the total widths, were kept fixed at the values in the literature (Tilley et al. 1998), as well as the energy and spin parity of each resonance. The $d^2\sigma/dE_{\mathrm{cm}}d\Omega_n$ best-fit cross section obtained from Equation (3) is shown together with the TH data in Figure 2 (middle red line, $\tilde{\chi}^2 = 2.1$). The top and bottom lines mark the upper and lower limits set by the statistical and normalization errors. A good fit is obtained without including non-resonant contributions.

Values of γ_p and γ_{α_0} from the fitting were then used to evaluate the resonance contribution to the on-energy-shell (OES) ^{19}F$(p,\alpha_0)^{16}$O astrophysical factor, according to standard *R*-matrix formulae. This is possible as in the modified *R*-matrix approach the same reduced widths appear as in the OES S(E)-factor, the only difference being the absence of any Coulomb or centrifugal penetration factor in the entrance channel (see Equation (3)). The OES S(E)-factor calculated with γ_p and γ_{α_0} in Table 1 is shown in Figure 3. Since the TH cross section provided the resonance contribution only, the non-resonant part of the cross section was taken from Angulo et al. (1999). The middle red curve represents the S(E)-factor obtained using the parameters from the best fit, while the red band arises from the uncertainties in the resonance parameters of the 12.957, 13.048, 13.222, 13.224, and 13.226 MeV ^{20}Ne states, namely the errors introduced in the present calculations (statistical + normalization).

The main result of the present work is the estimate of the contribution of the 12.957 MeV ^{20}Ne level to the total astrophysical factor, as it is responsible of a resonance at 113 keV, well inside the energy range of astrophysical interest. Moreover, a lower limit has been established for the contribution of the 13.222, 13.224, and 13.226 MeV ^{20}Ne states, to satisfy the

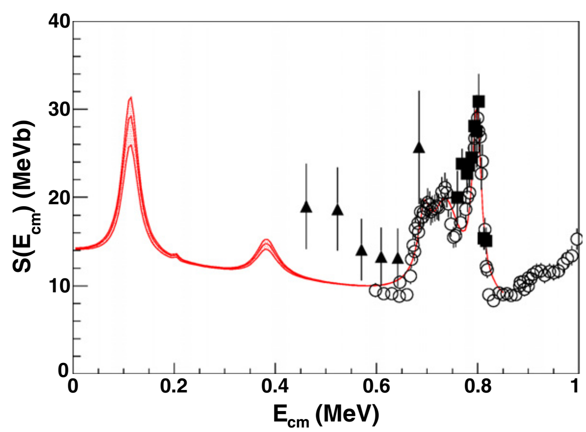

Figure 3. *R*-matrix parameterization of the ^{19}F$(p,\alpha_0)^{16}$O astrophysical factor. Above 0.6 MeV, the reduced partial widths were obtained through an *R*-matrix fit of direct data (open circles from Isoya et al. 1958, black squares from Caracciolo et al. 1974, black triangles from Breuer 1959). Below 0.6 MeV, the resonance parameters were obtained from the modified *R*-matrix fit (Figure 2). Values of γ_ps and γ_{α_0}s are all listed in Table 1. The non-resonant contribution is taken from Angulo et al. (1999). The curve obtained with the best-fit parameters is given by the middle line, the red band highlighting the region allowed by the uncertainties (statistical + normalization) on the fitting parameters (Table 1).

(A color version of this figure is available in the online journal.)

condition set by Lorentz-Wirzba (1978); Herndl et al. (1991); Yamashita & Kudo (1993), namely the dominance of direct reaction mechanism in the 0.14–0.6 MeV energy range. These levels yield resonances at ∼0.4 MeV, thus their role is marginal below 0.3 MeV, except if the strengths of the 13.222 and 13.224 MeV resonances were very large, which seems to be excluded within the errors of the direct data (Lorentz-Wirzba 1978; Herndl et al. 1991; Yamashita & Kudo 1993).

5. REACTION RATE AND CONCLUSIONS

The reaction rate *R* for the ^{19}F$(p,\alpha_0)^{16}$O reaction was calculated using the astrophysical factor in Figure 3 by means of standard equations (Rolfs & Rodney 1988; Iliadis 2007). The best-fit curve (middle line in Figure 3) was used and the upper and lower limits provided the uncertainty range. The results are displayed in Figure 4: in panel (a) the reaction

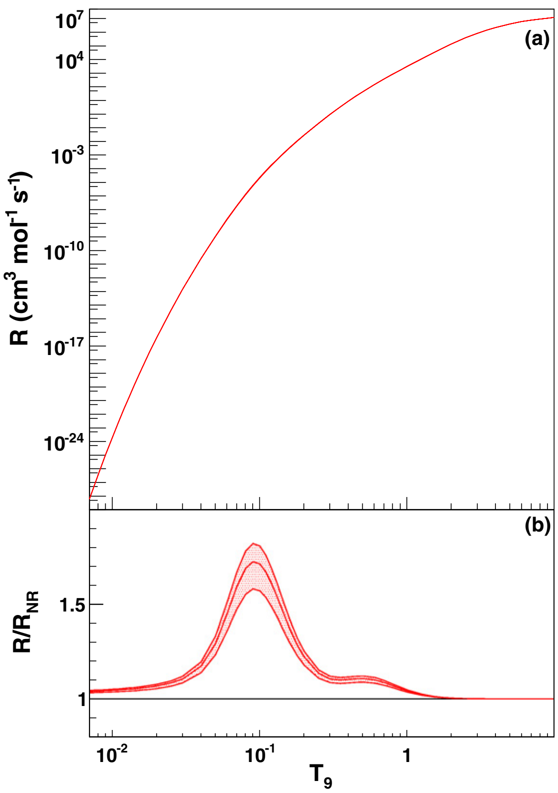

Figure 4. (a) Reaction rate for the ^{19}F$(p,\alpha_0)^{16}$O reaction calculated from the S(E)-factor in Figure 3. Upper and lower limits are also given, though they are barely visible because of the large rate range. (b) Ratio of the reaction rate in panel (a) to the rate of the ^{19}F$(p,\alpha_0)^{16}$O reaction evaluated following the prescriptions in Angulo et al. (1999). The red band arises from statistical and normalization errors.

(A color version of this figure is available in the online journal.)

rate in cm^3 mol^{-1} s^{-1} while in panel (b) its ratio to the one calculated following the NACRE prescription are shown. This was deduced assuming a non-resonant behavior of the S(E)-factor from 0.6 MeV downward, thus it will be referred to as the non-resonant reaction rate $R_{\rm NR}$. $R/R_{\rm NR}$ represents essentially the deviation of the ^{19}F$(p,\alpha_0)^{16}$O reaction rate obtained here from the one in the literature. For $T_9 \sim 0.1$ the reaction rate R largely departs from the non-resonant one, the difference being clearly due to the presence of the 113 keV resonance. The largest difference, about 70%, occurs at temperatures relevant for post-AGB stars, exceeding the upper limit set by the uncertainties in Angulo et al. (1999). The 13.226 MeV state in ^{20}Ne gives instead a small contribution to the total reaction rate, following the conclusions drawn in Lorentz-Wirzba (1978), Herndl et al. (1991), and Yamashita & Kudo (1993).

The energy resolution was not enough for achieving a good separation between resonances, especially at ~400 keV, thus preventing an accurate estimate of their total widths. Thus, the interesting results already achieved call for improved investigations in the full energy region with a better energy resolution to perform more accurate spectroscopy of the involved resonances.

A quantitative estimate of the impact of this measurement has been attempted. Following the suggestion in Lucatello et al. (2011) and Abia et al. (2011), we run parametric extra-mixing calculations according to the model in Busso et al. (2010); Palmerini et al. (2011) to evaluate to what extent the fluorine destructions varies if the NACRE reaction rate is replaced by the one obtained here. We found that the fluorine surface abundance can be depleted $\lesssim$40% more with respect to the NACRE rate in an $M = 2\,M_\odot$ and $Z = 10^{-4}$ AGB star. Since a significant fraction of fluorine upper limits for a sample of metal-poor AGB stars are located under the predicted values by a factor of the same order (Lucatello et al. 2011), this updated reaction rate can help to solve the fluorine puzzle in these stars in the framework of extra-mixing. In the $M = 2\,M_\odot$ and $Z = 10^{-4}$ AGB stellar model[9] used for preliminary calculations, the mixed material experiences temperatures up to $T_9 \sim 0.05$, where the reaction rate is 27% higher than in NACRE. An even larger destruction is expected in those environments where the reaction rate enhancement approaches a factor of 1.7 ($T_9 \sim 0.1$). Therefore, extensive calculations are undergoing to understand the consequences of the present results on astrophysics.

The work was supported in part by the Italian MIUR under grant No. RBFR082838.

A.M.M. acknowledges the support of the US DOE under grant No. DE-FG02-93ER40773 and DE-SC0004958 (topical collaboration TORUS), NSF Grant No. PHY-0852653.

V.B., V.K., Z.H., J.M., and Š.P. were supported by Czech MŠMT under Grant No. LC07050, Czech Academy grant No. M10480902, AMVIS Project grant No. LH1101, and GAČR. Project No. P203/10/310.

REFERENCES

Abia, C., Cunha, K., Cristallo, S., et al. 2010, ApJ, 715, L94
Abia, C., et al. 2011, ApJ, 737, L8
Angulo, C., Arnould, M., Rayet, M., et al. 1999, Nucl. Phys. A, 656, 3
Baur, G. 1986, Phys. Lett. B, 178, 135
Blatt, J. M., & Biedenharn, L. C. 1952, Rev. Mod. Phys., 24, 258
Breuer, G. 1959, Z. Phys., 154, 339
Busso, M., Palmerini, S., Maiorca, E., et al. 2010, ApJ, 717, L47
Caracciolo, R., et al. 1974, Lett. Nuovo Cimento, 11, 33
Cherubini, S., Kondratyev, V. N., Lattuada, M., et al. 1996, ApJ, 457, 855
Clayton, G. C., Geballe, T. R., Herwig, F., Fryer, C., & Asplund, M. 2007, ApJ, 662, 1220
Cristallo, S., Straniero, O., Gallino, R., et al. 2009, ApJ, 696, 797
Cuzzocrea, P., et al. 1980, Lett. Nuovo Cimento, 28, 515
Herndl, H., Abele, H., Staudt, G., et al. 1991, Phys. Rev. C, 44, R952
Iliadis, C. 2007, Nuclear Physics of Star (New York: Wiley-VCH)
Isoya, A., Ohmura, H., & Momota, T. 1958, Nucl. Phys., 7, 116
Jorissen, A., Smith, V. V., & Lambert, D. L. 1992, A&A, 261, 164
La Cognata, M., Goldberg, V. Z., Mukhamedzhanov, A. M., Spitaleri, C., & Tribble, R. E. 2009, Phys. Rev. C, 80, 012801
La Cognata, M., Romano, S., Spitaleri, C., et al. 2007, Phys. Rev. C, 76, 065804
La Cognata, M., Spitaleri, C., Mukhamedzhanov, A. M., et al. 2008, Phys. Rev. Lett., 101, 152501
La Cognata, M., Spitaleri, C., & Mukhamedzhanov, A. 2010a, ApJ, 723, 1512
La Cognata, M., Spitaleri, C., Mukhamedzhanov, A., et al. 2010b, ApJ, 708, 796
Lane, A. M., & Thomas, R. G. 1958, Rev. Mod. Phys., 30, 257
Lorentz-Wirzba, H. 1978, PhD thesis, Univ. Münster
Lucatello, S., Masseron, T., Johnson, J. A., Pignatari, M., & Herwig, F. 2011, ApJ, 729, 40
Lugaro, M., Ugalde, C., Karakas, A. I., et al. 2004, ApJ, 615, 934
Meynet, G., & Arnould, M. 2000, A&A, 355, 176
Morita, S., Nakagawa, T., Chu-Chung, H., & Sang-Mu, L. 1966, J. Phys. Soc. Japan, 21, 2435
Mukhamedzhanov, A., Blokhintsev, L. D., Brown, S., et al. 2007, Nucl. Phys. A, 787, 321
Mukhamedzhanov, A., Blokhintsev, L. D., Irgaziev, B. F., et al. 2008, J. Phys. G: Nucl. Part. Phys., 35, 014016
Nollett, K. M., Busso, M., & Wasserburg, G. J. 2003, ApJ, 582, 1036
Palmerini, S., La Cognata, M., Cristallo, S., & Busso, M. 2011, ApJ, 729, 3
Pandey, G., Lambert, D. L., & Kameswara Rao, N. 2008, ApJ, 674, 1068
Pizzone, R. G., Spitaleri, C., Lamia, L., et al. 2011, Phys. Rev. C, 83, 045801

9 Stellar parameters are taken from Cristallo et al. (2009).

Pizzone, R. G., Spitaleri, C., Mukhamedzhanov, A. M., et al. 2009, Phys. Rev. C, 80, 025807
Rolfs, C., & Rodney, W. S. 1988, Cauldrons in the Cosmos (Chicago, IL: Univ. Chicago Press)
Sergi, M. L., Spitaleri, C., La Cognata, M., et al. 2010, Phys. Rev. C, 82, 032801
Spitaleri, C., Aliotta, M., Cherubini, S., et al. 1999, Phys. Rev. C, 60, 055802
Spyrou, K., Chronidou, C., Harissopulos, S., et al. 2000, Eur. Phys. J. A, 7, 79
Tilley, D. R., Cheves, C. M., Kelley, J. H., Raman, S., & Weller, H. R. 1998, Nucl. Phys. A, 636, 247
Warsh, K. L., Temmer, G. M., & Blieden, H. R. 1963, Phys. Rev., 13, 1690
Woosley, S. E., & Haxton, W. C. 1988, Nature, 334, 45
Yamashita, Y., & Kudo, Y. 1993, Prog. Theor. Phys., 90, 1303